

Research Article

## Adsorption Isotherms and Kinetic Studies of Methylene Blue Removal by *Jatropha curcas* Seeds

W.N.E.M. Nazeri<sup>a</sup>, S.M. Puzi<sup>a\*</sup>, A.F. Osman<sup>a</sup>, H. Haroon<sup>a</sup>, S.A. Adnan<sup>a</sup>, N.H.A. Zaidi<sup>a</sup>, M.N.I. Jamaludin<sup>b</sup>

<sup>a</sup> Faculty of Chemical Engineering & Technology, Universiti Malaysia Perlis, Perlis, Malaysia

<sup>b</sup> Institute of Autonomous System, Universiti Teknologi Petronas, Perak, Malaysia

### ARTICLE INFO

#### Article History:

Received 14 September 2025

Received in revised form 31 March 2026

Accepted 1 April 2026

Available online 30 June 2026

#### Keywords:

Adsorption Isotherms,  
Kinetic,  
Methylene blue,  
*Jatropha curcas* seeds

### ABSTRACT

This study investigates the potential of *Jatropha curcas* seed as a low-cost biosorbent for the removal of methylene blue (MB) from aqueous solutions. The biosorbent was prepared through drying, grinding, and sieving processes, followed by characterization using Scanning Electron Microscopy (SEM) and Fourier Transform Infrared (FTIR) spectroscopy. Batch adsorption experiments were conducted to evaluate the effects of initial dye concentration, pH, adsorbent dosage, and contact time. The optimum conditions were identified at pH 11, initial concentration of 50 mg/L, and adsorbent dosage of 1.0 g, achieving a maximum removal efficiency of 77.15% and adsorption capacity of 6.17 mg/g. The adsorption process was best described by the Langmuir isotherm and pseudo-second-order kinetic model, indicating monolayer adsorption and chemisorption mechanism. The findings demonstrate that *Jatropha curcas* seeds are a promising sustainable biosorbent for wastewater treatment applications.

©UTM Penerbit Press. All rights reserved

### INTRODUCTION

Industrialization and urbanization significantly contributed to the release of pollutants into water bodies, leading to the degradation of water quality and posing serious environmental and public health risks (Ahmed et al., 2020). Among these pollutants, synthetic dyes were a major concern, as they were widely used in industries such as textiles, paper, plastics, and pharmaceuticals (Mokif, 2019). Methylene blue (MB), a commonly used cationic dye, was extensively utilized in dyeing processes due to its vivid colour and stability. However, its presence in wastewater posed significant challenges, as it was toxic, non-biodegradable, and harmful to aquatic life and human health, causing issues such as respiratory problems and skin irritation.

The discharge of untreated or inadequately treated dye-containing effluents into water bodies resulted in aesthetic pollution, reduced light penetration, and disruption of aquatic ecosystems (Periyasamy, 2024). Even at low concentrations, MB exhibited harmful effects, making its removal from wastewater a critical environmental priority. Various conventional methods were employed for dye

removal, including chemical precipitation, coagulation, flocculation, oxidation, membrane filtration, and biological treatment (Ledakowicz & Pázdziór 2021). While these methods were effective, they often had limitations, such as high operational costs, complex procedures, and the generation of secondary waste requiring additional treatment (Ledakowicz & Pázdziór 2021). These drawbacks highlighted the need for more sustainable, cost-effective, and environmentally friendly alternatives.

Among emerging technologies, adsorption gained considerable attention due to its simplicity, affordability, and high efficiency in removing dyes from wastewater (Velusamy et al., 2021). Adsorption involves the adhesion of dye molecules onto the surface of an adsorbent material. Researchers increasingly focused on natural materials and agricultural by-products as low-cost and eco-friendly adsorbents.

One promising approach is biosorption, a technology that uses biological materials, known as biosorbents, to

\*Corresponding Author

E-mail address: [svazwanimahmad@unimap.edu.my](mailto:svazwanimahmad@unimap.edu.my)

DOI address: 10.11113/bioprocessing.v5n1.78

ISBN/©UTM Penerbit Press. All rights reserved

remove pollutants such as dyes and heavy metals from wastewater (Torres, 2020). Biosorption relies on the ion-exchange capabilities of living-organism-derived materials (Velusamy et al., 2021). Examples of biosorbents include bacteria, yeast, seaweed, rice husk, and other biomaterials. This method has attracted significant research interest due to its low cost and high effectiveness. However, biosorption remains in developmental stages, with ongoing studies to enhance its performance. The preparation of biosorbents is particularly critical, as it significantly impacts their adsorption efficiency.

*Jatropha curcas*, a drought-resistant plant commonly cultivated in tropical and subtropical regions, has been identified as a potential biosorbent (Anoop & Premkumar, 2022). Its seeds, often considered agricultural waste, possess a porous structure and functional groups capable of binding with dye molecules. Utilizing *Jatropha curcas* seeds for MB removal not only provided an eco-friendly solution but also aligned with the principles of waste valorization by converting agricultural residues into valuable resources.

Despite the increasing number of studies exploring agricultural biomass as biosorbents, limited attention has been given to the adsorption performance of *Jatropha curcas* seed, particularly in relation to adsorption isotherms and kinetic behavior. Furthermore, the relationship between physicochemical properties and adsorption performance remains insufficiently discussed.

Therefore, this study aims:

1. To prepare *Jatropha curcas* seed as a biosorbent
2. To characterize the biosorbent using SEM and FTIR techniques.
3. To evaluate the effects of operational parameters (initial concentration, pH, adsorbent dosage, and contact time) on MB adsorption.
4. To analyze adsorption behavior using isotherm and kinetic models.

## MATERIALS AND METHOD

### Materials

MB (analytical grade), sodium hydroxide (NaOH), and hydrochloric acid (HCl) were obtained from Merck (Germany). Distilled water was used throughout the experiments.

### Preparation of *Jatropha curcas* Seeds

The *Jatropha curcas* seeds were initially exposed to sunlight to effectively eliminate surface moisture. After that, they were placed in an oven set at 105 °C for 24 hours to ensure thorough drying and the complete removal of moisture that could interfere with the subsequent liquefaction process (Kenedi & Marchetti, 2019). Once dried, the seeds were allowed to cool to ambient temperature before proceeding to the next stage. The outer layer of the seeds was manually removed, leaving only the seed kernels. These kernels were then ground into a fine powder using a grinder, and the resulting powder was stored in a clean container to prevent contamination.

### Characterization

Surface morphology was analysed using Scanning Electron Microscopy (SEM, COXEM EM-30AX, South Korea). Functional groups were identified using Fourier Transform Infrared Spectroscopy (FTIR, PerkinElmer Spectrum 65, USA) using the KBr pellet method.

### Preparation of MB Solution

A stock solution of 1000 mg/L MB was prepared and diluted to obtain concentrations ranging from 10 to 50 mg/L. Absorbance measurements were conducted using a UV-Vis spectrophotometer (Shimadzu UV-1800, Japan) at 665 nm.

### Batch Adsorption Experiment

Batch adsorptions were conducted to determine the adsorption isotherms and kinetics parameters. In this experiment, MB solutions of the desired concentrations were prepared by diluting the previously prepared stock solution. Each solution was placed in an Erlenmeyer flask and transferred to an incubator shaker, which was set to operate at a temperature of 30 °C and an agitation speed of 150 rpm (Yusop et al., 2021). After the designated contact time, the samples were filtered to remove any remaining adsorbent. The absorbance of the filtrates was then measured at a wavelength of 665 nm using a UV-vis spectrometer. Equilibrium data were recorded when the contact time reached 180 minutes, providing the basis for analysing the adsorption performance and kinetics. The determination of optimum conditions was conducted sequentially. Initially, the effect of initial dye concentration was evaluated, and the concentration yielding the highest adsorption performance (50 mg/L) was selected. Subsequently, the effect of pH was studied using this concentration, and the optimal pH (pH 11) was identified. These optimum values were then applied in subsequent experiments, including adsorbent dosage and contact time studies, to ensure consistency and comparability of results.

### Effect of Initial Concentrations

The experiment was performed using MB solutions with initial concentrations ranging from 10 mg/L to 50 mg/L, specifically 10 mg/L, 20 mg/L, 30 mg/L, 40 mg/L, and 50 mg/L. For each concentration, 200 mL of the solution was added to Erlenmeyer flasks containing 0.1 g of *Jatropha curcas* seeds. The mixtures were maintained at an optimal pH and a temperature of 30 °C while being agitated at 150 rpm. Samples were collected at 30-minute intervals and continued until equilibrium was achieved. The concentration yielding the highest adsorption efficiency was selected as the optimum concentration for analysing the subsequent study parameters.

### Effect of pH

The effect of pH on the adsorption of MB onto *Jatropha curcas* seeds was studied over a pH range of 3 to 11, including pH values of 3, 5, 7, 9, and 11 (Loutfi et al., 2023). The pH of the dye solution was adjusted using 0.1 M sodium hydroxide (NaOH) or 0.1 M hydrochloric acid (HCl), with a pH meter used to ensure accurate adjustment. A MB solution with an initial concentration of 40 mg/L was mixed with 0.1 g of *Jatropha curcas* seeds and agitated at 150 rpm and 30 °C for varying time intervals. After agitation, the samples were filtered, and their absorbance was measured. The pH that demonstrated the highest adsorption efficiency was identified and selected for further analysis.

### Effect of Adsorbent Mass

To investigate the effect of adsorbent mass on adsorption, experiments were conducted using varying quantities of *Jatropha curcas* seeds. In 250 mL flasks, 200 mL of MB solution at the optimal concentration and pH were mixed with 0.1 g, 0.3 g, 0.5 g, 0.7 g, and 1.0 g of *Jatropha curcas*

seeds (Uddin, 2020). The experiments were carried out at a constant agitation speed of 150 rpm and a temperature of 30 °C. The absorbance of the dye solutions was measured at 30-minute intervals using a UV-vis spectrometer set to a wavelength of 665 nm.

#### Effect of Contact Time

The experiments were conducted using all the most optimal parameter values. Samples were collected at 30-minute intervals until the dye concentration absorbance stabilized and remained constant.

#### Adsorption Calculation

The efficiency of dye removal was assessed by calculating both the percentage removal and the adsorption capacity (Al-Ghouti & Al-Absi, 2020). These calculations were performed using Equations (1) and (2) respectively:

$$R (\%) = \frac{C_i - C_e}{C_i} \times 100 \quad (1)$$

$$q_e = \frac{C_i - C_e}{m} \times V \quad (2)$$

where R represent the percentage removal of dyes,  $q_e$  is the equilibrium adsorption capacity of dyes (mg/g),  $C_i$  is the initial dye concentration (mg/L),  $C_e$  represents the equilibrium dye concentration (mg/L), V is the volume of the dye solution (L), and m is the mass of the adsorbent used (g).

#### Adsorption Isotherms

The adsorption behaviour of MB onto *Jatropha curcas* seeds biosorbent was analysed using two widely applied isotherm models which are the Freundlich and Langmuir isotherms (Rápo & Tonk, 2021).

#### Freundlich Isotherm

Equation (3) can be linearized by taking logarithms on both sides:

$$q_e = K_F C_e^{\frac{1}{n}} \quad (3)$$

Equation (3) can be linearized by taking logarithms on both sides:

$$\log q_e = \log K_F + \frac{1}{n} \log C_e \quad (4)$$

Where  $q_e$  is the amount of dye absorbed per unit of adsorbent,  $C_e$  is dye concentration at equilibrium,  $K_F$  and n are Freundlich constants which can be determined from the intercept and slope of Freundlich plot respectively.

#### Langmuir isotherm

$$q_e = \frac{q_m K_L C_e}{1 + K_L C_e} \quad (5)$$

Equation (5) can be linearized:

$$\frac{1}{q_e} = \frac{1}{q_m} + \frac{1}{K_L q_m C_e} \quad (6)$$

Where  $q_m$  is the maximum adsorption amount with complete monolayer coverage on adsorbent surface,  $C_e$  is the dye concentration at equilibrium,  $K_L$  is the Langmuir

constant. The value of  $q_m$  and  $K_L$  can be determine from the Langmuir linear plot  $\frac{1}{C_e}$  against  $\frac{1}{q_e}$ .

#### Adsorption Kinetics Models

Adsorption kinetics models were analysed using Pseudo-first-order and pseudo-second-order kinetic models (Uddin & Nasar, 2020).

#### Pseudo-First-Order Kinetic Model

This model assumes that the rate at which the solute is adsorbed over time is directly proportional to the difference between the saturation concentration and the amount of solute adsorbed onto the solid at a specific time. The relationship is described using the linearized Equation (7) provided below:

$$\log (q_e - q_t) = \log q_e - \frac{k_1 t}{2.303} \quad (7)$$

Where  $q_t$  is the amount of dye adsorbed per unit of adsorbent (mg/g), t is the contact time (min) and  $k_1$  is the pseudo-first-order constant which can be determined from the plot of  $\log (q_e - q_t)$  against t.

#### Pseudo-Second-Order Kinetic Model

This kinetic model can be represented by Equation (8):

$$\frac{dq_t}{dt} = k_2 (q_e - q_t)^2 \quad (8)$$

Integrating Equation (8) with  $q_t = 0$  at  $t = 0$ , a linearized Equation (9) is obtained:

$$\frac{1}{q_t} = \frac{1}{k_2 q_e^2} + \frac{t}{q_e} \quad (9)$$

Where  $k_2$  is the pseudo-second-order rate constant ( $g \text{ mg}^{-1} \text{ min}^{-1}$ ).  $q_e$  and  $k_2$  can be obtained by linear plot of  $t/q_t$  versus t.

## RESULTS AND DISCUSSION

#### Surface Morphology Before and After Biosorption

The surface morphology of *Jatropha curcas* seeds at magnifications of 500× and 1000× is presented in Figure 1 (i) and (ii). Prior to adsorption, the SEM images reveal that the biosorbent surface is rough, irregular, and highly porous. These structural characteristics are advantageous for adsorption, as they provide a large surface area and abundant active sites for dye molecules.

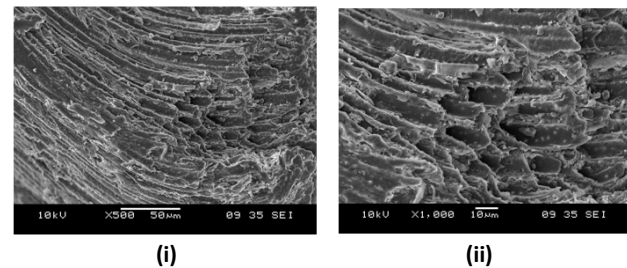
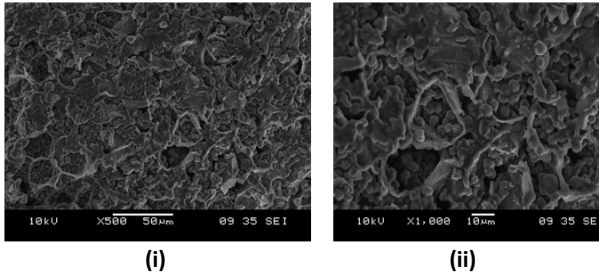
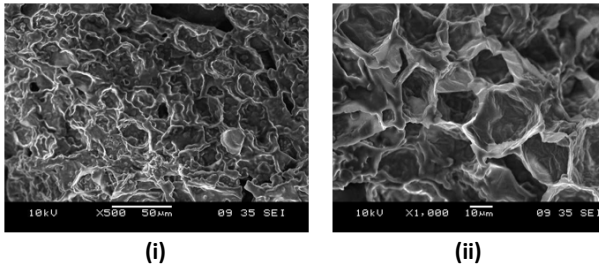


Figure 1 *Jatropha curcas* seeds surface before adsorption at (i) magnification x500 and (ii) magnification x1000



**Figure 2** Surface morphology of *Jatropha curcas* seeds after adsorption at an initial MB concentration of 50 mg/L (magnification: (i) 500×, (ii) 1000×)



**Figure 3** Surface morphology of *Jatropha curcas* seeds after adsorption at pH 11 (magnification: (i) 500×, (ii) 1000×)

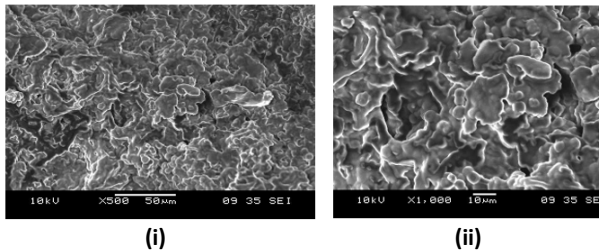


**Figure 4** Surface morphology of *Jatropha curcas* seeds after adsorption at an adsorbent dosage of 1.0 g (magnification: (i) 500×, (ii) 1000×)

The presence of pores in the biosorbent can be classified into micropores, mesopores, and macropores, which collectively contribute to enhanced adsorption performance by facilitating mass transfer and diffusion of MB molecules into the internal structure of the biosorbent (Al-Ghouti & Al-Absi, 2020; Rápó & Tonk, 2021). Similar porous and heterogeneous surface structures have been widely reported in lignocellulosic biomass used for dye adsorption (Velusamy et al., 2021).

After the biosorption process, the SEM images shown in Figures 2, 3, and 4 indicate significant changes in surface morphology under different operating conditions. The surface appears smoother and less porous compared to the raw biosorbent. This observation suggests that MB molecules have been successfully adsorbed onto the surface and within the pores of the biosorbent.

The reduction in pore visibility and surface roughness can be attributed to the occupation of active sites and pore channels by dye molecules, leading to pore filling and surface coverage (Uddin & Nasar, 2020). This phenomenon is commonly observed in adsorption studies, where the adsorbent surface undergoes morphological changes after interaction with pollutants (Abdallah & Alprol, 2024).

Furthermore, the differences observed in SEM images under varying conditions of initial concentration, pH, adsorbent dosage, and contact time indicate that adsorption behavior is influenced by operating parameters. At optimal

conditions, more uniform surface coverage is observed, suggesting efficient adsorption and stronger interaction between MB molecules and the biosorbent surface.

Overall, the SEM analysis confirms that *Jatropha curcas* seed possesses a suitable porous structure for adsorption and undergoes significant morphological changes after biosorption, providing strong evidence for the effectiveness of this material as a biosorbent.

**Functional Group of Biosorbent**

From Figure 5, there are six main peaks has been observed. The six main peaks were detected at wavelength of 3414.83  $cm^{-1}$ , 2922.81  $cm^{-1}$ , 1638.36  $cm^{-1}$ , 1421.03  $cm^{-1}$ , 1060.00  $cm^{-1}$ , and 618.97  $cm^{-1}$  respectively. These peaks indicate the presence of specific functional groups on the surface of *Jatropha curcas* seeds, as shown in Table 1.

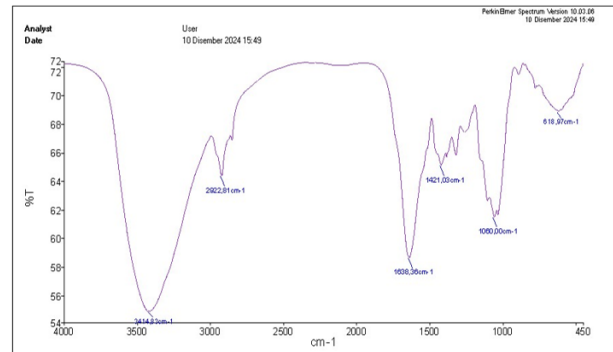


**Figure 5** FTIR spectrum of *Jatropha curcas* seeds before biosorption

**Table 1** Functional groups present in *Jatropha curcas* seeds before biosorption.

Wavelength ( $cm^{-1}$ )	Functional Group	Functional Class	Intensity
3414.83	O-H (Hydroxyl)	Alcohols/Phenols	Strong
2922.81	C-H (Alkyl)	Alkanes	Medium
1638.36	C=O (Carbonyl)	Esters/Carboxylic	Medium
1421.03	C-H (Alkyl)	Alkanes	Medium
1060.00	C-O (Alcohols)	Alcohols/Ethers	Medium
618.97	C-H ( $CH_2$ )	Alkanes	Weak

The FTIR spectrum of *Jatropha curcas* seeds revealed the presence of several functional groups that contribute significantly to the adsorption of MB. The broad peak observed at approximately 3414.83  $cm^{-1}$  corresponds to O–H stretching vibrations, which are commonly associated with hydroxyl groups present in lignocellulosic biomass. These groups play an important role in adsorption through hydrogen bonding interactions with dye molecules (Velusamy et al., 2021; Torres, 2020).

The peak at 2922.81  $cm^{-1}$  is attributed to C–H stretching vibrations of aliphatic chains, indicating the presence of alkyl groups. These groups may contribute to hydrophobic interactions between the biosorbent and dye molecules (Rápó & Tonk, 2021). The peak observed at 1638.36  $cm^{-1}$  corresponds to C=O stretching vibrations, representing carbonyl functional groups, which can interact electrostatically with cationic dye molecules such as MB (Al-Ghouti & Al-Absi, 2020).

Furthermore, the peak at 1421.03  $cm^{-1}$  is associated with C–H bending vibrations, while the peak at 1060.00  $cm^{-1}$  is attributed to C–O stretching vibrations of alcohols or

ethers. These functional groups enhance adsorption through dipole–dipole and van der Waals interactions (Uddin & Nasar, 2020). The weak peak at  $618.97\text{ cm}^{-1}$  corresponds to out-of-plane bending of C–H bonds, which may indicate the presence of aromatic structures contributing to adsorption sites (Pudza & Abidin, 2020).

Overall, the presence of hydroxyl, carbonyl, and alkyl functional groups suggests that *Jatropha curcas* seeds possess multiple active sites capable of adsorbing MB through hydrogen bonding, electrostatic attraction, and hydrophobic interactions.

The FTIR spectrum after adsorption, as shown in Figure 6, indicates noticeable changes in peak positions and intensities. Six main peaks were observed at  $3420.22$ ,  $3937.01$ ,  $1743.54$ ,  $1451.21$ ,  $1163.01$ , and  $720.45\text{ cm}^{-1}$ , suggesting modifications in the chemical environment of the functional groups after biosorption.

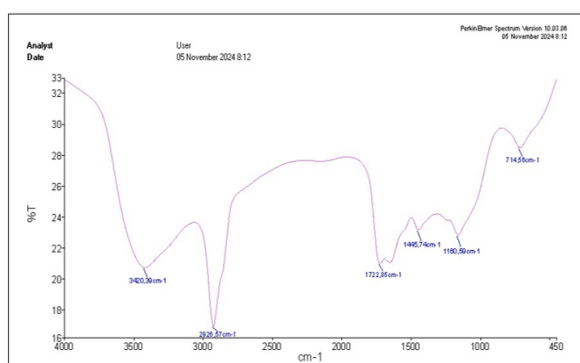


**Figure 6** FTIR spectrum of *Jatropha curcas* seeds after biosorption.

The slight shift of the O–H peak from  $3414.83\text{ cm}^{-1}$  to  $3420.22\text{ cm}^{-1}$  indicates changes in hydrogen bonding interactions, suggesting involvement of hydroxyl groups in the adsorption process (Velusamy et al., 2021). The appearance of a new peak at  $3937.01\text{ cm}^{-1}$  may be associated with enhanced interactions between the adsorbent surface and dye molecules, possibly due to changes in surface chemistry after adsorption. The functional group are shown in Table 2 below.

**Table 2** Functional groups present in *Jatropha curcas* seeds after biosorption.

Wavelength ( $\text{cm}^{-1}$ )	Functional Group	Functional Class	Intensity
3420.22	O-H (Hydroxyl)	Alcohols/Phenols	Strong
3937.01	C-H (Alkyl)	Alkanes	Medium
1743.54	C=O (Carbonyl)	Esters/Carboxylic	Medium
1451.21	C-H (Alkyl)	Alkanes	Medium
1163.01	C-O (Alcohols)	Alcohols/Ethers	Medium
720.45	C-H ( $\text{CH}_2$ )	Alkanes	Weak

The shift of the carbonyl peak from  $1638.36\text{ cm}^{-1}$  to  $1743.54\text{ cm}^{-1}$  indicates the participation of C=O groups in the adsorption mechanism, likely through electrostatic interactions with the cationic dye (Al-Ghouti & Al-Absi, 2020). Similarly, the shift in C–H bending vibrations from  $1421.03\text{ cm}^{-1}$  to  $1451.21\text{ cm}^{-1}$  suggests structural modifications in the biosorbent matrix following dye adsorption.

The appearance of a new peak at  $1163.01\text{ cm}^{-1}$  corresponding to C–O stretching indicates the involvement of alcohol or ether groups in adsorption interactions. Additionally, the peak at  $720.45\text{ cm}^{-1}$  suggests possible interactions between MB molecules and aromatic structures on the biosorbent surface (Rápó & Tonk, 2021).

These spectral changes confirm that functional groups present in *Jatropha curcas* seeds actively participate in the adsorption of MB. The shifts in peak positions and the emergence of new peaks provide strong evidence of chemical interactions between the dye molecules and the biosorbent surface, supporting a chemisorption mechanism.

### Effect of Initial Dye Concentration on Biosorption

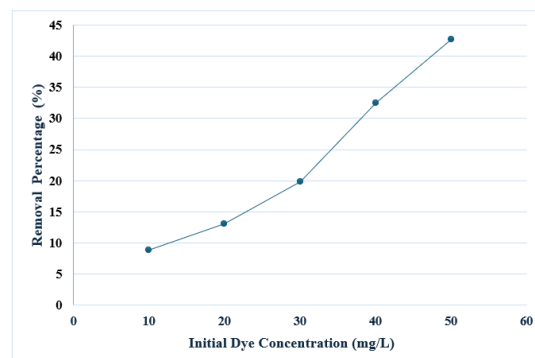
The effect of initial dye concentration on biosorption was investigated using  $0.1\text{ g}$  of *Jatropha curcas* seeds with dye concentrations ranging from  $10$  to  $50\text{ mg/L}$  at  $30\text{ }^\circ\text{C}$ . Figure 7(i) illustrates the effect of initial dye concentration on percentage removal, while Figure 7(ii) shows the corresponding adsorption capacity.

As shown in Figure 7(i), the percentage of dye removal increased with increasing initial dye concentration. This behaviour can be attributed to the role of initial concentration as a driving force for mass transfer between the aqueous solution and the biosorbent surface (Rápó & Tonk, 2021). At higher concentrations, a greater concentration gradient is established, which enhances the diffusion of MB molecules onto the surface of *Jatropha curcas* seeds.

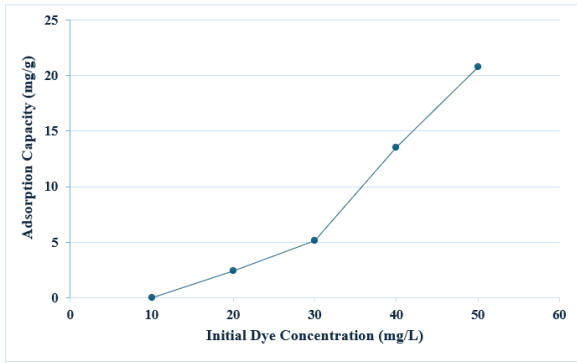
Similarly, Figure 7(ii) indicates that the adsorption capacity increased with increasing initial dye concentration. This is because a higher number of dye molecules are available to interact with the active sites on the biosorbent surface, leading to increased uptake per unit mass of adsorbent (Abdallah & Alprol, 2024).

However, it is important to note that although removal efficiency increased within the studied range, at sufficiently higher concentrations, a decrease in removal efficiency may occur due to the saturation of available adsorption sites. Since the adsorbent dosage remains constant, the number of active binding sites is limited. As the initial dye concentration increases, competition among dye molecules for these sites becomes more significant, which may eventually reduce the overall removal percentage.

Based on the results, the highest removal efficiency and adsorption capacity were obtained at  $50\text{ mg/L}$ . Therefore, this concentration was selected for subsequent adsorption studies. A similar trend has been reported for MB adsorption onto *Jatropha curcas* seeds, where increasing dye concentration enhances the driving force for adsorption and improves adsorption capacity (Pudza & Abidin, 2020).

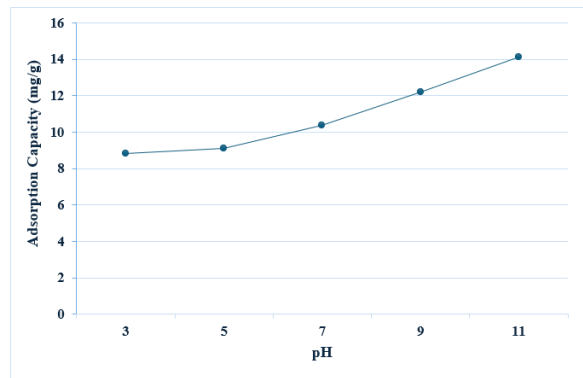


(i)



(ii)

**Figure 7** Effect of initial dye concentration on (i) removal percentage, (ii) adsorption capacity at equilibrium (0.1 g *Jatropha curcas* seeds, 30 °C, 150 rpm)

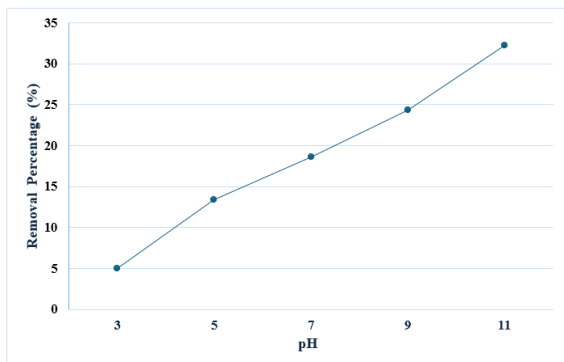


(ii)

**Figure 8** Effect of pH on (i) removal percentage, (ii) adsorption capacity at equilibrium (50 mg/L, 0.1 g *Jatropha curcas* seeds, 30 °C, 150 rpm)

**Effect of pH**

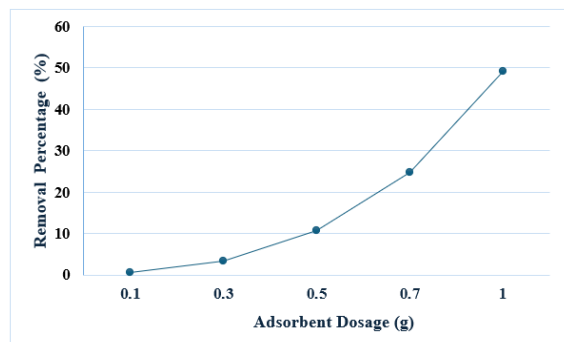
The pH of the MB solution plays a crucial role in influencing the adsorption efficiency. It can affect the surface charges of the biosorbent, the degree of ionization, and the characteristics of the adsorbate (Al-Ghouthi & Al-Absi, 2020; Rápó & Tonk, 2021). As shown in the graphs in Figure 8 (i) and (ii), both the removal percentage and adsorption capacity increase with the initial pH of the dye solution. The highest removal percentage (33.24%) and adsorption capacity (14.11 mg/g) are achieved when the initial pH of the solution is 11. These results indicate that *Jatropha curcas* seed performs better in adsorbing MB in an alkaline solution. FTIR analysis of the *Jatropha curcas* seed reveals the presence of several anionic functional groups on its surface. At lower pH, protonation of these functional groups occurs, causing them to carry a positive charge, which limits the adsorption of cationic MB (Mantasha et al., 2020). At higher pH, less protonation takes place, making the anionic functional groups available to attract the cationic dye. Consequently, pH 11 was chosen for the study of subsequent parameters. However, research by Taha et al. (2024) was done in their study, both adsorption capacity and removal percentage increased as pH increased from 3 to 7 but decreased when the pH increased from 7 to 11. This difference is attributed to the distinct functional groups present on *Jatropha curcas* seedcake compared to *Jatropha curcas* seeds. Researcher explained that as the pH increased from 2 to neutral, the repulsive forces between the adsorbent decreased, enhancing dye removal (Taha et al., 2024). However, at higher pH levels, hydrolysis occurs, resulting in positive charges on the surface of the adsorbent itself (Taha et al., 2024).



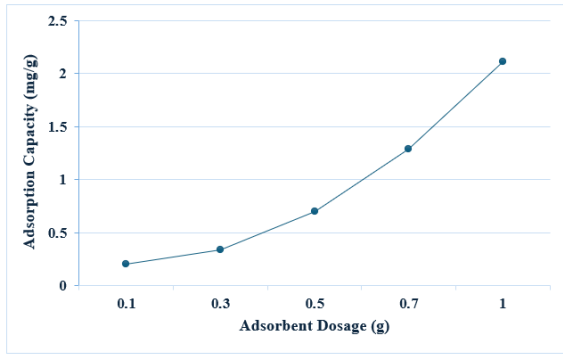
(i)

**Effect of Biosorbent Dosage on Biosorption**

Figure 9 illustrates the effect of biosorbent dosage on the change in dye concentration. From the graphs in Figure 9(i) and (ii), it is observed that the increase in biosorbent dosage increases both the percentage of dye removal and adsorption capacity. The percentage removal of MB by *Jatropha curcas* seed increased from 0.69% to 49.18% by increasing the dosage adsorbent. Same as the adsorption capacity which increased from 0.20 mg/g to 2.12 mg/g. This is because higher dosages will expose more pores or active sites on the biosorbent, allowing more MB to be adsorbed onto the rambutan seed. As a result, it results in the removal of more MB from the solution, hence a higher percentage removal. Additionally, the amount of dye particles adsorbed per gram of *Jatropha curcas* seed increases, hence increased adsorption capacity. Previous studies have examined the influence of adsorbent dosage on adsorption performance, showing that increasing the biosorbent mass significantly enhances MB uptake using *Jatropha curcas* seeds (Pudza & Abidin, 2020). The adsorption capacity was reported to increase from 11.47 to 82.05 mg/g as the biosorbent dosage increased from 0.25 g to 1.5 g. This behavior is attributed to the increased availability of active binding sites and surface area at higher dosages, which promotes greater interaction between dye molecules and the biosorbent. Additionally, higher adsorbent dosage reduces competition among dye molecules for adsorption sites, thereby improving overall adsorption efficiency.



(i)

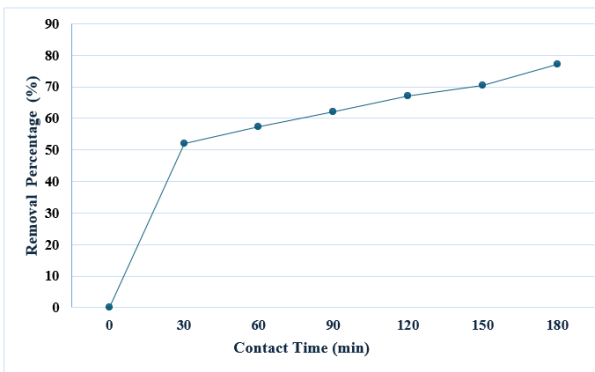


(ii)

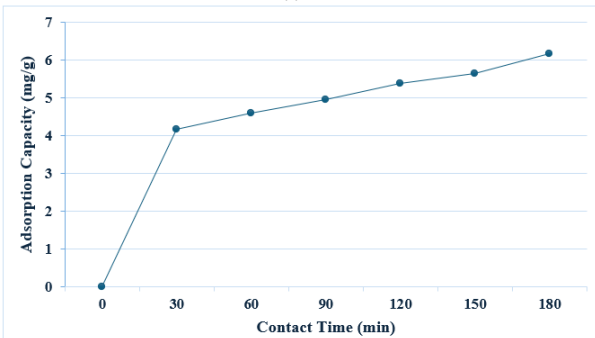
**Figure 9** Effect of biosorbent dosage on (i) removal percentage, (ii) adsorption capacity at equilibrium (50 mg/L, pH 11, 30 °C, 150 rpm)

**Effect of Contact Time on Biosorption**

The study of the change in dye concentration over time was studied using 50 mg/L of MB solution at pH 11 with 1.0 g of *Jatropha curcas* seeds at temperature of 30 °C. It can be seen from **Figure 10 (i)** that the removal percentage increases with contact time up to 30 minutes because of the biosorption of MB onto the *Jatropha curcas* seeds. As the biosorption proceeds, the removal of MB from the dye solution occurs simultaneously. The maximum percentage removal reaches 77.15% at equilibrium. **Figure 10 (ii)** shows the quantity of dye adsorbed per gram of *Jatropha curcas* seed. Adsorption capacity increases and reaches a maximum of 6.17mg/g at equilibrium, where it is assumed that all available pores on the biosorbent are saturated with adsorbed dye particles (Al-Ghouti & Al-Absi, 2020).



(i)

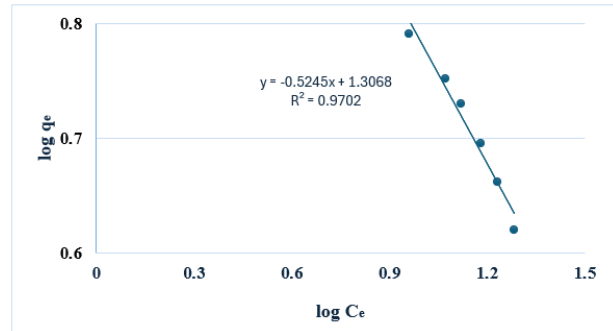


(ii)

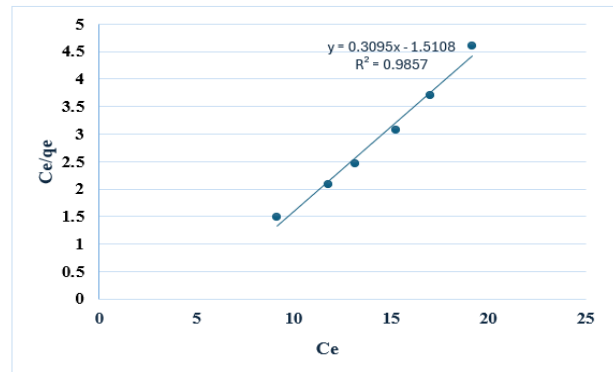
**Figure 10** Effect of contact time on (i) removal percentage, (ii) adsorption capacity at equilibrium (50 mg/L, pH 11, 1 g of *Jatropha curcas* seeds, 30 °C and 150 rpm)

**Adsorption Isotherms Study**

The Freundlich and Langmuir isotherms are plotted in **Figure 11**.



(i)



(ii)

**Figure 11** Adsorption isotherms (i) Freundlich isotherm (ii) Langmuir isotherm

Based on **Figure 11**, it can be concluded that the Langmuir isotherm provides a better fit for describing the adsorption of MB onto *Jatropha curcas* seed, as its  $R^2$  value is closer to 1 as show in **Table 3**. This suggests that MB molecules are adsorbed onto the *Jatropha curcas* seed surface as a monolayer on a homogeneous surface. Furthermore, there is no stacking of MB particles, indicating that the adsorption process is limited to surface coverage only (Taha et al., 2024).

**Table 3** Important value for Freundlich and Langmuir isotherms

Freundlich isotherm	Langmuir isotherm
$R^2 = 0.9702$	$R^2 = 0.9857$
$K_F = 20.27$	$K_L = 0.66 \text{ L/mg}$
$n = 1.91$	$q_m = 3.23 \text{ mg/g}$

**Kinetic Models**

Pseudo-first and second order kinetics models are plotted as **Figure 12** to find out the most suitable adsorption mechanism utilized by *Jatropha curcas* seed to adsorb the MB.

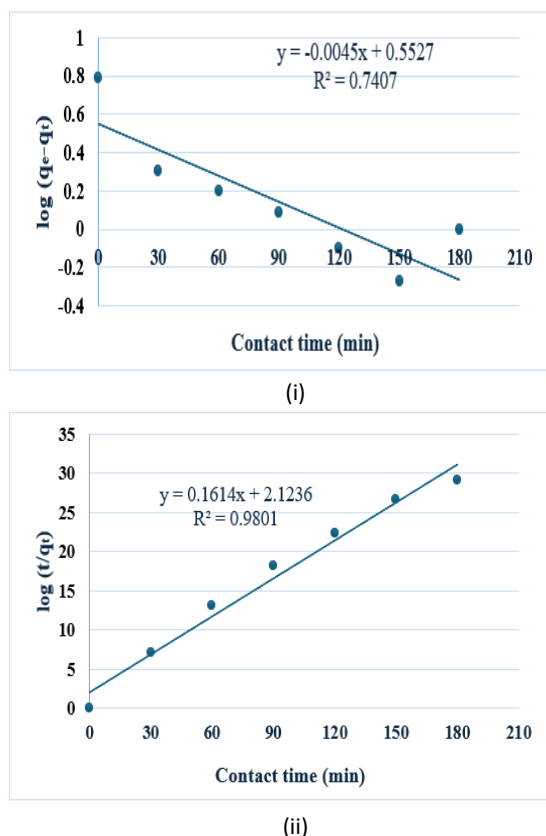


**Figure 12** Kinetic models (i) Pseudo-first-order model (ii) Pseudo-second order-model.

The  $R^2$  value for the pseudo-second-order model was found to be 0.9801, which is significantly closer to 1 compared to the pseudo-first-order model with an  $R^2$  value of 0.7407 as reported in **Table 4**. This indicates that the pseudo-second-order kinetic model provides a better fit to describe the adsorption mechanism. The adsorption of MB onto *Jatropha curcas* seed is therefore more likely to follow a chemisorption process rather than physisorption. This suggests that the adsorption mechanism may involve the formation of covalent bonds between functional groups present in MB and those on the surface of *Jatropha curcas* seed (Taha et al., 2024).

**Table 4** Important values of pseudo-first order and pseudo-second-order kinetic models

Pseudo-first-order model	Pseudo-second-order model
$R^2 = 0.7407$	$R^2 = 0.9801$
$k_1 = 0.0103$	$k_2 = 0.0012$

## CONCLUSION

This study addressed the need for low-cost and sustainable adsorbents for dye removal by investigating the potential of *Jatropha curcas* seed as a biosorbent. The biosorbent was successfully prepared and characterised using SEM and FTIR analyses, which confirmed the presence of functional groups and porous structures suitable for adsorption. Batch adsorption experiments demonstrated that operational parameters significantly influence adsorption performance, with optimum conditions identified at pH 11, initial concentration of 50 mg/L, and adsorbent dosage of 1.0 g.

Under these conditions, a maximum removal efficiency of 77.15% and adsorption capacity of 6.17 mg/g were achieved. The adsorption process followed the Langmuir isotherm and pseudo-second-order kinetic model, indicating monolayer adsorption and chemisorption mechanism. These findings highlight the potential of *Jatropha curcas* seed as an effective and environmentally friendly biosorbent. Future studies are recommended to explore regeneration capability, adsorption of multiple pollutants, and large-scale application feasibility.

## References

- Abdallah, M. A. M. & Alprol, A. E. (2024). Utilization of aquatic biomass as biosorbent for sustainable production of high surface area, nano- microporous, for removing two dyes from wastewater. *Scientific Reports*, 14(1). <https://doi.org/10.1038/s41598-024-54539-2>
- Ahmed, T., Zounemat-Kermani, M., & Scholz, M. (2020). Climate change, water quality and water-related challenges: A review with focus on Pakistan. In *International Journal of Environmental Research and Public Health* (Vol. 17, Issue 22, pp. 1–22). MDPI AG. <https://doi.org/10.3390/ijerph17228518>
- Al-Ghouti, M. A. & Al-Absi, R. S. (2020). Mechanistic understanding of the adsorption and thermodynamic aspects of cationic methylene blue dye onto cellulosic olive stones biomass from wastewater. *Scientific Reports*, 10(1). <https://doi.org/10.1038/s41598-020-72996-3>
- Anoop, M. & Premkumar, G. (2022). Bioenergy through bioelectricity in an integrated bioreactor-bioelectricity generator system for phenol biodegradation. In *Bioenergy Crops* (pp. 215–226). CRC Press. <https://doi.org/10.1201/9781003043522-12>
- Keneni, Y. G. & Marchetti, J. M. (2019). Temperature and pretreatment effects on the drying of different collections of *Jatropha curcas* L. seeds. *SN Applied Sciences*, 1(8). <https://doi.org/10.1007/s42452-019-0969-3>
- Ledakowicz, S. & Pázdziór, K. (2021). Recent achievements in dyes removal focused on advanced oxidation processes integrated with biological methods. *Molecules*, 26(4). <https://doi.org/10.3390/molecules26040870>
- Loutfi, M., Mariouch, R., Mariouch, I., Belfaquir, M., & ElYoubi, M. S. (2023). Adsorption of methylene blue dye from aqueous solutions onto natural clay: Equilibrium and kinetic studies. *Materials Today: Proceedings*, 72, 3638–3643. <https://doi.org/10.1016/j.matpr.2022.08.412>
- Mantasha, I., Saleh, H. A. M., Qasem, K. M. A., Shahid, M., Mehtab, M., & Ahmad, M. (2020). Efficient and selective adsorption and separation of methylene blue (MB) from mixture of dyes in aqueous environment employing a Cu(II) based metal organic framework. *Inorganica Chimica Acta*, 511. <https://doi.org/10.1016/j.ica.2020.119787>
- Mokif, L. A. (2019). Removal methods of synthetic dyes from industrial wastewater: A review. *Mesopotamia Environmental Journal*, 5(1), 23–40. <https://doi.org/10.31759/mej.2019.5.1.0040>
- Periyasamy, A. P. (2024). Recent advances in the remediation of textile-dye-containing wastewater:

- prioritizing human health and sustainable wastewater treatment. In *Sustainability (Switzerland)* (Vol. 16, Issue 2). Multidisciplinary Digital Publishing Institute (MDPI). <https://doi.org/10.3390/su16020495>
- Pudza, M. Y. & Abidin, Z. Z. (2020). A sustainable and eco-friendly technique for dye adsorption from aqueous media using waste from *Jatropha curcas* (Isotherm and kinetic model). *Desalination and Water Treatment*, 182, 365–374. <https://doi.org/10.5004/dwt.2020.25169>
- Rápó, E. & Tonk, S. (2021). Factors affecting synthetic dye adsorption; desorption studies: A review of results from the last five years (2017–2021). In *Molecules* (Vol. 26, Issue 17). MDPI. <https://doi.org/10.3390/molecules26175419>
- Taha, Z. S., Labena, A., Madian, H. R., Ahmed, H. S., & Hassan, H. M. (2024). Promising applications of seedcake of *Jatropha curcas* plants: Bioethanol production and bio-sorbent material for dye and heavy metal removal. *Biomass Conversion and Biorefinery*, 14(10), 11601–11615. <https://doi.org/10.1007/s13399-022-03193-7>
- Torres, E. (2020). Biosorption: A review of the latest advances. In *Processes* (Vol. 8, Issue 12, pp. 1–23). MDPI AG. <https://doi.org/10.3390/pr8121584>
- Uddin, M. K. & Nasar, A. (2020). Walnut shell powder as a low-cost adsorbent for methylene blue dye: isotherm, kinetics, thermodynamic, desorption and response surface methodology examinations. *Scientific Reports*, 10(1). <https://doi.org/10.1038/s41598-020-64745-3>
- Velusamy, S., Roy, A., Sundaram, S., & Kumar Mallick, T. (2021). A review on heavy metal ions and containing dyes removal through graphene oxide-based adsorption strategies for textile wastewater treatment. In *Chemical Record* (Vol. 21, Issue 7, pp. 1570–1610). John Wiley and Sons Inc. <https://doi.org/10.1002/tcr.202000153>
- Yusop, M. F. M., Ahmad, M. A., Rosli, N. A., & Manaf, M. E. A. (2021). Adsorption of cationic methylene blue dye using microwave-assisted activated carbon derived from acacia wood: Optimization and batch studies. *Arabian Journal of Chemistry*, 14(6). <https://doi.org/10.1016/j.arabjc.2021.103122>